pathways not influenced by normal molecules (*24*). Multiple pathways may lead to MEK activation. The protein product expressed by the *MEK* cDNA should facilitate additional studies of this pathway.

REFERENCES AND NOTES

1. C. M. Crews, A. Alessandrini, R. L. Erikson, *Cell Growth Differ.* **3**, 135 (1992); M. H. Cobb, T. G. Boulton, D. J. Robbins, *Cell Regul.* **2**, 965 (1991); S. L. Pelech, J. S. Sanghera, M. Daya-Makin, *Biochem. Cell. Biol.* **68**, 1297 (1990); G. Thomas, *Cell* **68**, 3 (1992); T. W. Sturgill and J. Wu, *Biochim. Biophys. Acta* **1092**, 350 (1991).
2. C. M. Crews and R. L. Erikson, *Proc. Natl. Acad. Sci. U.S.A.* **89**, 8205 (1992).
3. S. Matsuda *et al.*, *EMBO J.* **11**, 973 (1992).
4. N. Gómez and P. Cohen, *Nature* **353**, 170 (1991).
5. J. M. Kyriakis *et al.*, *ibid.* **358**, 417 (1992).
6. R. Seger *et al.*, *J. Biol. Chem.* **267**, 14373 (1992).
7. A. Alessandrini, C. M. Crews, R. L. Erikson, *Proc. Natl. Acad. Sci. U.S.A.* **89**, 8200 (1992).
8. Degenerate oligonucleotide primers were synthesized on the basis of amino acid sequence of two peptides recovered from a tryptic digest of purified MEK (*2*). Primer AC1, CGAATTCC(T/G)(T/C)TC(A/C/T/G)GG(A/C/T/G)(C/G)(T/A)CAT (A/G)TA (512 possible permutations), based on peptide 4 (*2*), and primer AC3, CCGAATTCCA(T/C)GA (A/G)TG(T/C)(T/A)(G/C)(A/C/G/T)CC (256 possible permutations), based on peptide 2, were used in a PCR (50 μl) containing 20 mM deoxynucleotide triphosphates, primers AC1 and AC3 (10 mm), 1× Promega Taq buffer, 1 unit of Taq polymerase, and a sample of lambda gt10 murine pre–B cell library 22D6 (provided by D. Schatz, Yale University), representing approximately 6.4 × 10^4 plaque-forming units. Thirty cycles of denaturation at 94°C for 1 min, annealing at 50°C for 1 min and extension at 72°C for 1 min were preceded by 3 min at 94°C to disrupt the phage particles and followed by 7 min at 72°C for a final extension. The resulting heterogeneous 300- to 500-bp product was reamplified for 25 cycles under the same conditions as above but at 60°C annealing temperature and without the initial 3-min denaturation step. The resulting heterogeneous 300- to 500-bp product from this amplification was used as a template for a PCR with primers AC1 and AC2—CGAATTCTG(T/C)TTT(A/T)(G/C)(C/A/G)CC(A/C/G/T)TA(T/C)AT (T/C/A)G. Both primers AC2 and AC3 encode segments of peptide 2 (*2*); however, the AC2 sequence is COOH-terminal to AC3. Therefore, AC2 can be used in a PCR with AC3:AC1 PCR products as starting template. Twenty-five PCR cycles under similar conditions at 30°C annealing temperature yielded a single band of approximately 350 bp. This PCR product was digested with Eco RI, subcloned into Bluescript SK+ and sequenced by the dideoxynucleotide method. The 228-bp insert was then labeled by the random oligonucleotide-primed method and used to screen 1 × 10^6 plaques of a cDNA library made from 22D6 pre–B cells. Hybridization was performed for 24 hours at 37°C in a solution of 30% formamide, 0.6 M NaCl, 0.075 M sodium citrate, 0.065 M KH_2PO_4, 1× Denhardt's solution (0.02% each of bovine serum albumin, Ficoll, and polyvinylpyrrolidone), 0.5% SDS, heat-denatured salmon sperm DNA (100 μg/ml), and heat-denatured probe (3 × 10^5 cpm/ml). The filters were washed for 2 hours at 37°C in 0.3 M NaCl, 0.03 M sodium citrate, 0.1% SDS. ^{32}P was detected by autoradiography, and 39 putative clones were obtained. Five clones were inserted into pBS-SK+ and further analyzed by sequencing by dideoxynucleotide chain termination. One of the longest clones, designated 4-3, was used for further analysis.
9. M. Kozak, *J. Cell Biol.* **108**, 229 (1989).
10. A. Alessandrini, unpublished data.
11. S. K. Hanks, A. M. Quinn, T. Hunter, *Science* **241**, 42 (1988).
12. S. A. Nadin-Davis and A. Nasim, *EMBO J.* **7**, 985 (1988).
13. G. Boguslawski and J. O. Polazzi, *Proc. Natl. Acad. Sci. U.S.A.* **84**, 5848 (1987); M. A. Teague, D. T. Chaleff, B. Errede, *ibid.* **83**, 7371 (1986).
14. T. Toda, M. Shimanuki, M. Yanagida, *Genes Dev.* **5**, 60 (1991); W. E. Courchesne, R. Kunisawa, J. Thorner, *Cell* **58**, 1107 (1989); E. A. Elion, P. L. Grisafi, G. R. Fink, *ibid.* **60**, 649 (1990).
15. D. E. Levin, F. O. Fields, R. Kunisawa, J. M. Bishop, J. Thorner, *Cell* **62**, 213 (1990).
16. O. Nielsen, J. Davey, R. Egel, *EMBO J.* **11**, 1391 (1992).
17. B. J. Stevenson, N. Rhodes, B. Errede, G. F. Sprague, Jr., *Genes Dev.* **6**, 1293 (1992).
18. S. M. Thomas, M. DeMarco, G. D'Arcangelo, S. Halegoua, J. S. Brugge, *Cell* **68**, 1 (1992).
19. K. W. Wood, C. Sarnecki, T. M. Roberts, J. Blenis, *ibid.*, p. 1041.
20. Y. Wang, H.-P. Xu, M. Riggs, L. Rodgers, M. Wigler, *Mol. Cell. Biol.* **11**, 3554 (1991).
21. B. R. Cairns, S. W. Ramer, R. D. Kornberg, *Genes Dev.* **6**, 1305 (1992).
22. S. K. Gupta, C. Gallego, G. L. Johnson, L. E. Heasley, *J. Biol. Chem.* **267**, 7987 (1992).
23. J. C. Lacal *et al.*, *Science* **238**, 533 (1987); A. Wolfman, I. G. Macara, *Nature* **325**, 359 (1987).
24. A. M. M. de Vries-Smits, B. M. T. Burgering, S. J. Leevers, C. J. Marshall, J. L. Bos, *Nature* **357**, 602 (1992).
25. T. Maniatis, E. F. Fritsch, J. Sambrook, *Molecular Cloning: A Laboratory Manual* (Cold Spring Harbor Laboratory, Cold Spring Harbor, NY, 1982).
26. K.-L. Guan and J. E. Dixon, *Anal. Biochem.* **192**, 262 (1991).
27. C. M. Crews, A. A. Alessandrini, R. L. Erikson, *Proc. Natl. Acad. Sci. U.S.A.* **88**, 8845 (1991).
28. M. D. Adams *et al.*, *Nature* **355**, 632 (1992).
29. H. Kosako *et al.*, *EMBO J.* **11**, 2903 (1992).
30. H. Devereux, P. Haeberli, O. Smithies, *Nucleic Acids Res.* **12**, 387 (1984).

31. We thank M. Lim for his determined assistance with the sequence analysis and L. Scott for help with computer analysis, figures, and polishing the manuscript. Supported by NIH grant CA42580 (R.L.E.) and NIH Genetics Training Grant GM07620-14 (C.M.C.). R.L.E. is an American Cancer Society Professor of Cellular and Developmental Biology.

18 August 1992; accepted 18 September 1992

Removal of Nonhomologous DNA Ends in Double-Strand Break Recombination: The Role of the Yeast Ultraviolet Repair Gene *RAD1*

Jacqueline Fishman-Lobell* and James E. Haber†

Double-strand breaks (DSBs) in *Saccharomyces cerevisiae* can be repaired by gene conversions or by deletions resulting from single-strand annealing between direct repeats of homologous sequences. Although *rad1* mutants are resistant to x-rays and can complete DSB-mediated mating-type switching, they could not complete recombination when the ends of the break contained approximately 60 base pairs of nonhomology. Recombination was restored when the ends of the break were made homologous to donor sequences. Additionally, the absence of *RAD1* led to the frequent appearance of a previously unobserved type of recombination product. These data suggest *RAD1* is required to remove nonhomologous DNA from the 3′ ends of recombining DNA, a process analogous to the excision of photodimers during repair of ultraviolet-damaged DNA.

We have developed an approach to study recombination in vivo by examining DNA extracted from cells in which a galactose-inducible HO endonuclease was used to synchronously induce DSB recombination (*1*). Normally, the HO endonuclease initiates a site-specific intrachromosomal gene conversion event at the *MAT* locus (*2–4*). In addition to following *MAT* switching (*5*), we have examined DSB-induced homologous recombination in several constructs in which the HO endonuclease cut site was inserted into other genes (*6–9*). We have shown that in plasmids containing direct repeats of a homologous sequence, HO-induced DSBs are repaired through two kinetically separable pathways: a nonconservative single-strand annealing (SSA) mechanism that produces a deletion product (Fig. 1A) and gene conversion events that are not accompanied by reciprocal crossing-over (Fig. 1B) (*9*). With this system we have now examined the role that the ultraviolet (UV) excision repair gene *RAD1* (*10–12*) plays in these two pathways. Although *RAD1* has been principally implicated in the excision repair of UV photodimers, it also is involved in mitotic recombination, especially in the formation of deletions between repeated sequences (*13–16*).

A comparison of the kinetics of HO-induced recombination of plasmid pJF6 (Fig. 1C) is shown for wild-type and *rad1* strains in Fig. 2A. In wild-type strains, deletions and gene conversions are formed efficiently. In contrast, the *rad1* derivative showed no detectable gene conversion product and a fourfold reduction in the amount of deletion product (*17*). A genetic analysis (Table 1A) further substantiates the physical data. HO

Rosenstiel Basic Medical Sciences Research Center and Department of Biology, Brandeis University, Waltham, MA 02254.

*Present address, Harvard Medical School, Brigham and Womens Hospital, Boston, MA 02115.
†To whom correspondence should be addressed.

induction in *rad1* caused a dramatic loss of the *URA3*-containing plasmid pJF6. Those plasmids that were retained were mostly Lac$^+$, indicating that recombination was completed in some cases.

When the HO cut site was inserted in the promoterless copy of lacZ, pJFL23 (Fig. 1D), the *rad1* strain was again defective in the completion of recombination (Table 1C and Fig. 2, B and C). The 3.0-kb band indicative of gene conversions was absent (Fig. 2B), and only a small amount of the 6.8-kb band indicative of a deletion was detected (Fig. 2C). Identical results were also obtained when the two copies of lacZ were in inverted orientation, in plasmid pJF5 [Table 1B and Southern (DNA) blot analysis (*18*)].

We also found that *rad1* mutants prevented deletions that are formed between two *URA3* repeats that flank a chromosomally integrated HO cut site (Fig. 1F) (6, 8). Although deletion formation was nearly 100% efficient in wild-type strains, the induction of HO in *rad1* derivatives proved to be lethal. Only 7% (5 out of 70) of the cells were viable after HO induction and produced a deletion product, compared to

Table 1. Fate of LacZ plasmid after HO induction. Colonies were assayed for maintenance of both the *URA3* lacZ plasmid and the TRP1 GAL::HO plasmid before and after induction of the HO endonuclease. Those colonies that contained both plasmids were examined for their lacZ phenotype in X-gal assays. Strains tJL53-6, tJL53-5, tJL53-23, and tJL53-33 are wild-type strains carrying plasmids (**A**) pJF6, (**B**) pJF5, (**C**) pJFL23, and (**D**) pJFL33, respectively. Strains tJL10-5, tJL10-6, tJL10-23, and tJL10-33 are *rad1* strains carrying plasmids (A) pJF6, (B) pJF5, (C) pJFL23, and (D) pJFL33, respectively. The structures of pJF6, pJFL23, and pJFL33 are shown in Fig. 1, C through E, and pJF5 contains the lacZ genes in an inverted orientation with the HO cut site embedded in one of the lacZ genes.

	Strain	Plasmid	Rad1	Before HO induction			After HO induction		
				Trp$^+$	Trp$^+$Ura$^+$	LacZ$^+$	Trp$^+$	Trp$^+$Ura$^+$	LacZ^{+*}
A	tJL53-6	pJF6	+	85% 270/317	91% 246/270	2% 6/246	70% 285/406	85% 242/285	91% 220/242
	tJL10-6	pJF6	–	78% 261/333	78% 204/261	2% 3/139	44% 129/292	12% 15/129	80% 12/15
B	tJL53-5	pJF5	+	95% 125/132	90% 112/125	3% 3/112	63% 92/147	25% 23/92	96% 22/23
	tJL10-5	pJF5	–	87% 79/91	77% 61/79	3% 2/61	52% 76/146	8% 6/76	66% 4/6
C	tJL53-23	pJFL23	+	85% 103/121	92% 95/103	NA†	76% 102/135	75% 76/102	NA†
	tJL10-23	pJFL23	–	87% 123/141	90% 111/123	NA†	48% 98/204	14% 14/98	NA†
D	tJL53-33	pJFL33	+	84% 102/122	94% 96/102	NA†	67% 114/170	74% 84/114	NA†
	tJL10-33	pJFL33	–	92% 101/110	85% 86/101	NA†	44% 118/271	60% 71/118	NA†

*Lac$^+$/total Trp$^+$Ura$^+$ colonies. †The LacZ assay is not applicable to these plasmids, which contain either disruptions in both lacZ genes or a disruption only in the promoterless lacZ gene.

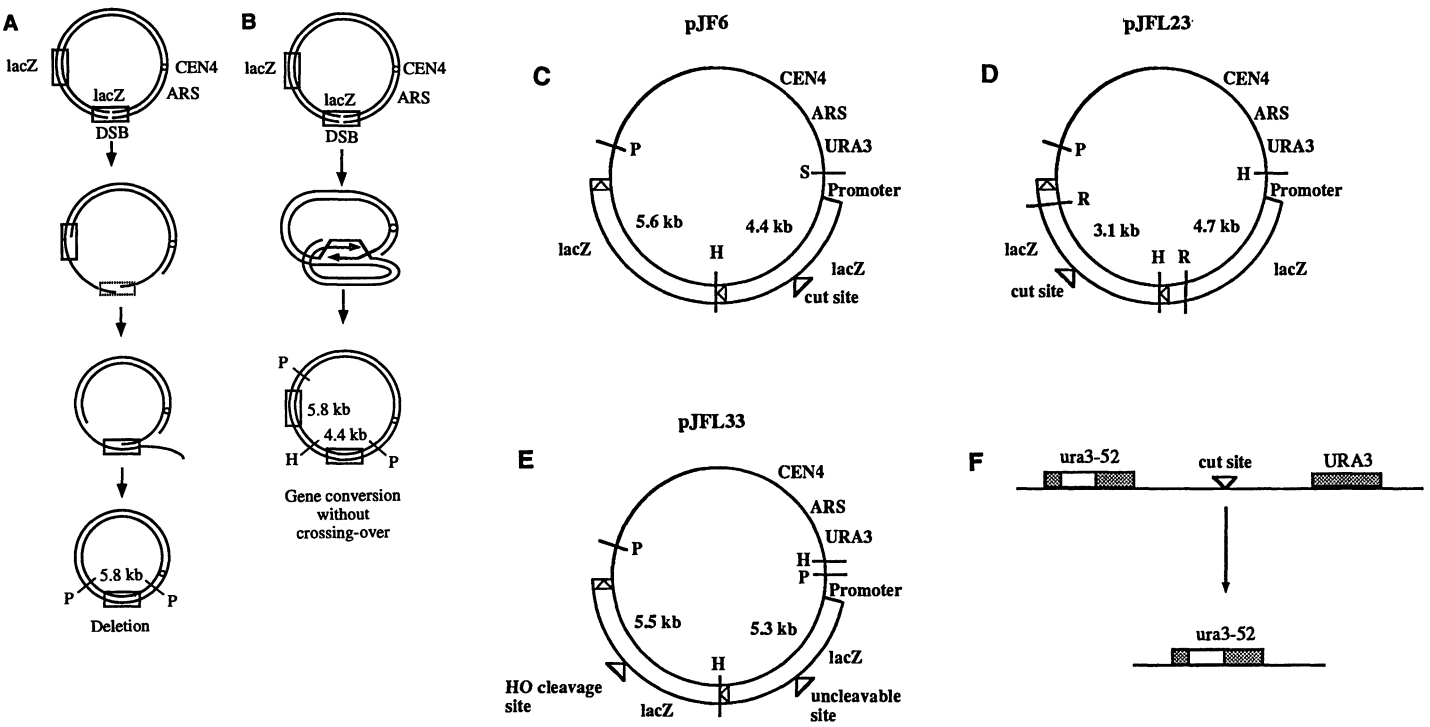

Fig. 1. The gap repair and the SSA models of DSB-initiated recombination. (**A**) In the SSA mechanisms, 5′–3′ degradation occurs at the ends of a break and continues until complementary homologous directly repeated regions become single-stranded. The complementary strands then anneal. (**B**) In the gap repair model, the 3′ ends of the break become single-stranded by a 5′–3′ exonuclease. The single-stranded ends invade a homologous duplex and fill the gap by DNA synthesis. (**C**) Structure of plasmid pJF6 containing a direct repeat of lacZ sequences. A transcribed lacZ gene is interrupted by the insertion of a 117-bp *MAT***a** HO endonuclease cut site. The second lacZ gene lacks a promoter but contains wild-type sequences. (**D**) Substrate pJFL23, which is the same as pJF6 except the HO cut site was inserted into the promoterless lacZ gene. (**E**) Substrate pJFL33 contains 117-bp *MAT* fragments in each lacZ gene. One contains wild-type sequences and is cut by the HO endonuclease, whereas the other contains a point mutation within the cut site and is no longer cleavable. (**F**) Chromosomal substrate for HO-induced events. The HO endonuclease cut site was inserted between two *URA3* repeats. After induction of a DSB, a deletion is formed between two *URA3* sequences. The sizes of relevant restriction fragments are indicated. Abbreviations for restriction enzyme sites shown are Pst I (P), Hind III (H), Sma I (S), and Eco RI (R). Additional sites for these enzymes exist but are not shown.

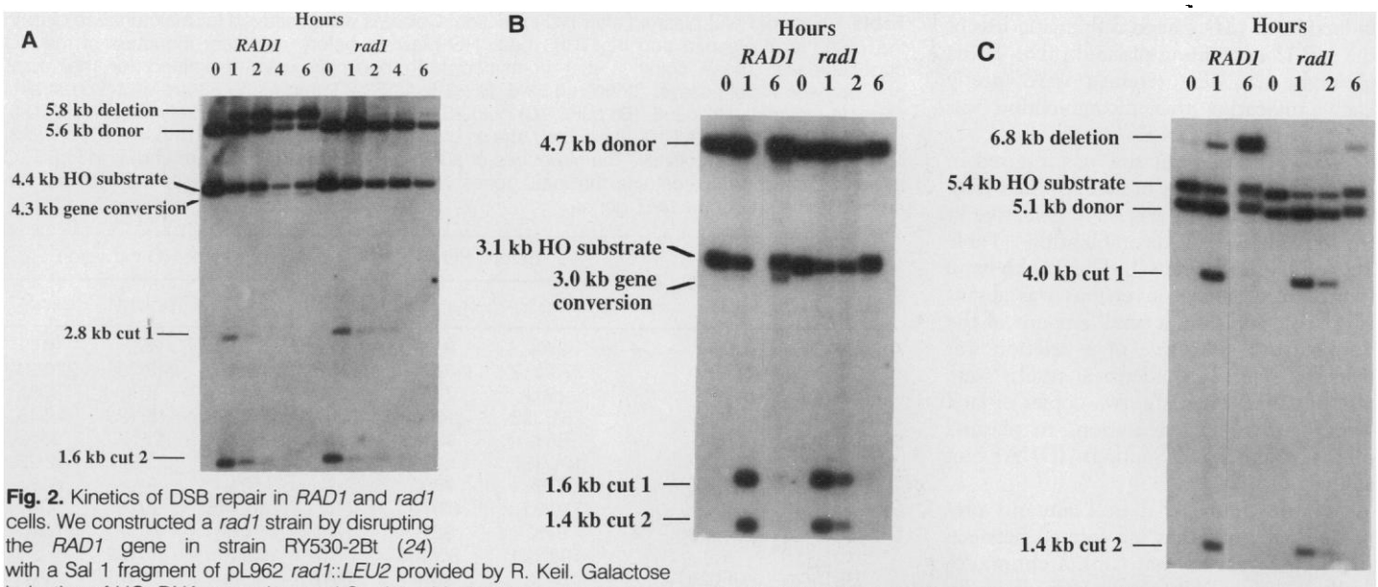

Fig. 2. Kinetics of DSB repair in *RAD1* and *rad1* cells. We constructed a *rad1* strain by disrupting the *RAD1* gene in strain RY530-2Bt (*24*) with a Sal 1 fragment of pL962 *rad1*::*LEU2* provided by R. Keil. Galactose induction of HO, DNA extraction, and Southern blotting were as described (*9*). (**A**) Autoradiogram of a time-course experiment from both wild-type (tJL53-6) and *rad1* (tJL10-6) strains containing pJF6. The 5.8-kb Pst I deletion product and the 4.3-kb Hind III–Sma I gene conversion product are efficiently produced in wild-type cells but are reduced or absent in the *rad1* strain. (**B**) and (**C**) Autoradiograms from wild-type and *rad1* strains containing pJFL23. In (B) DNA was digested with Hind III and Eco RI to show gene conversions. The 3.0-kb Hind III–Eco RI gene conversion product is produced in wild-type cells and is not detectable in the *rad1* mutant (*17*). In (C) DNA was digested with Pst I and Hind III to show the 6.8-kb Pst I–Hind III deletion product.

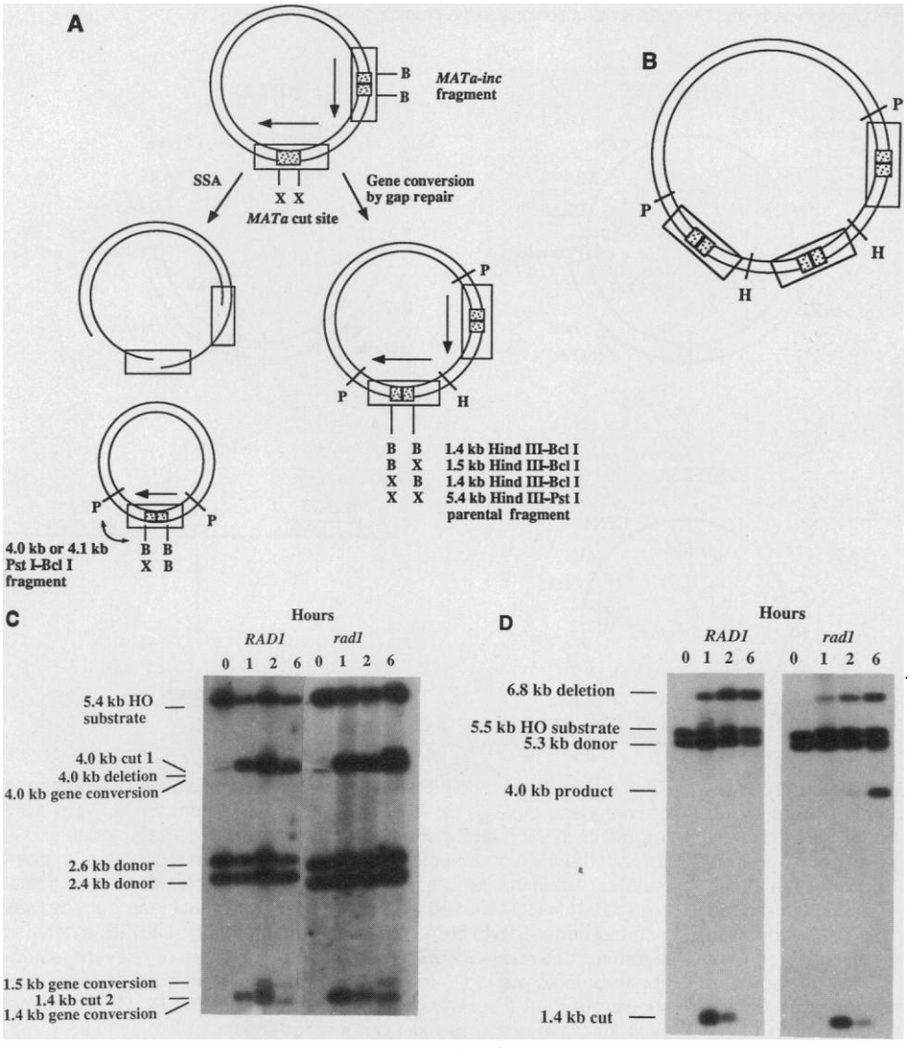

Fig. 3. Product formation in *RAD1* and *rad1* strains containing pJF33. (**A**) Diagram of this substrate indicating the position of the linkers and the products expected after recombination and mismatch repair. The position of relevant restriction sites for Pst I (P), Hind III (H), Bcl I (B), and Xho II (X) are shown. The insertion of the *MATa-inc* sequence (uncleavable by HO) into the Bcl I site of *lacZ* preserved the Bcl I sites, whereas the insertion of the cleavable segment carried Xho I sites. (**B**) A triplication produced in *rad1* cells. (**C**) After galactose induction of HO, DNA was digested with Pst I, Hind III, and Bcl I to examine gene conversion formation. Conversion of only the proximal site to Bcl I will produce a 1.5-kb Hind III–Bcl I fragment, whereas conversion of both sites to Bcl I will produce a 1.4-kb Hind III–Bcl I fragment. The 1.5-kb fragment of the gene conversion product is the only size fragment that uniquely represents this product. Although one of the HO-cut molecules is also 1.4 kb, the fragment persisting at 6 hours represents gene conversion because all of the HO cut DNA disappears by 6 hours (Figs. 2 and 3). (**D**) DNA digested with Pst I and Hind III to examine deletions. DNA was probed with *lacZ* sequences between Bsu 36I–Eco RV sites located 5′ to the inserted cut site. The 6.8-kb deletion product is produced efficiently in both wild-type and *rad1* strains. Additionally, a 4.0-kb fragment is produced in the *rad1* strain at the same time as the gene conversion product.

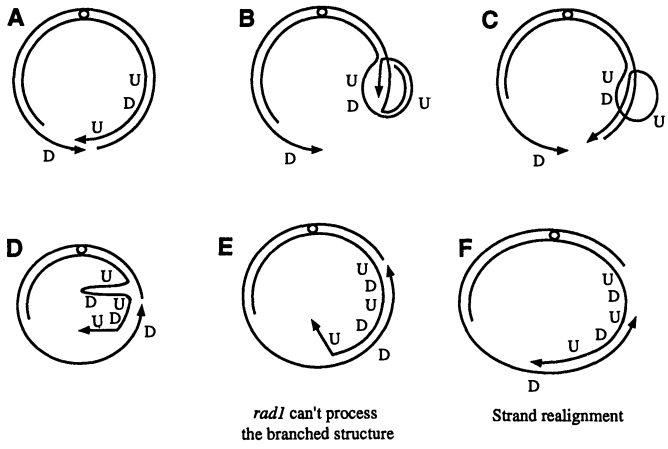

Fig. 4. A possible mechanism for the formation of triplications. After production of a DSB (**A**), the upstream end invades the upstream end of the donor gene (**B**) and repair synthesis occurs through the entire strand (**C**). This produces 2.5 units of lacZ on this strand. Invasion or pairing from the downstream end of the break with the newly synthesized strand (**D**) and repair synthesis produces a structure containing a tail. In wild-type cells, this tail can be removed, and repair synthesis fills in the plasmid, which produces a gene conversion product without crossing-over. The *rad1* strains cannot remove this tail (**E**), but denaturation and realignment of the annealed strands lead to homologous pairing of this tail. (**F**) Subsequent filling in by DNA repair synthesis produces a triplication.

93% (80 out of 86) for the wild-type control.

These results suggest that *RAD1* is required for the repair of HO-induced DSBs, although previous experiments have demonstrated that *rad1* mutants are only weakly sensitive to x-ray damage (*19*). We have confirmed that our *rad1*::*LEU2* deletion strain exhibits only a small increase in sensitivity to x-rays (*18*). Moreover, by introducing a *rad1*::*LEU2* deletion into strain R166, whose kinetics of *MAT* switching have been studied extensively (*5*, *20*), we also confirmed that the kinetics and efficiency of galactose-induced HO *MAT* switching are unaffected by *rad1*.

One essential difference between the HO-induced recombination of the lacZ plasmid substrates and either x-ray–induced DSB repair or *MAT* switching is that neither end of the DSB is homologous to the lacZ donor sequences with which recombination must take place. The lacZ substrates contain a 117-bp cutting site derived from *MAT***a** that must be removed. We postulated that *rad1* strains are unable to remove approximately 60 bp of nonhomologous DNA from either side of the DSB and that this failure blocks subsequent recombination. If this were so, one might restore recombination by inserting the missing homologous sequences into the lacZ donor sequence. We created such a substrate, pJFL33 (Fig. 1E), by the insertion of a single base pair mutation of the cleavage site that prevents HO cleavage, called *MAT***a**-*inc* (*21*).

HO-induced recombination of pJFL33 proved to be efficient in both wild-type and *rad1* strains (Table 1D). The conversion of the HO-cut DNA to donor DNA was detected by both the appearance of a 1.5-kb Hind III–Bcl I fragment and the persistence of a 1.4-kb Hind III–Bcl I fragment (Fig. 3). Gene conversion formation (Fig. 3C) was slower in the *rad1* mutant than in wild-type cells. Whether or not the ends were completely homologous to donor sequences did not alter the proportion of gene conversion products in wild-type cells (26% in pJFL33 versus 17% in pJF6 (*9*, *22*).

A physical analysis of deletion formation of pJFL33 shows that deletions were formed with the same kinetics in *rad1* mutants as in wild-type cells, although at a lower efficiency (*22*). Surprisingly, a new recombination product also appeared (Fig. 3D). A heretofore unobserved 4.0-kb band was produced with the same kinetics as the gene conversion product in the *rad1* strain. This band did not appear in wild-type cells. Further Southern blot analysis indicated that this band reflects the formation of a triplication of lacZ sequences (Fig. 3B). The identity of this structure was established by restriction digests with Hind III and with Pst I, which produced lacZ-homologous restriction fragments of 4.0 kb and 14.8 kb, respectively.

One could argue that requirements for homologous DNA ends in *rad1* strains might be explained by the absence of 5′ to 3′ exonuclease digestion, so that the internal lacZ homology is never revealed. We addressed this possibility by measuring 5′ to 3′ single-stranded DNA formation with dot blots of undenatured DNA (*8*, *9*). The formation of single-stranded DNA ending 3′ at the DSB was similar in *rad1* mutants and wild-type cells (*18*). These results suggest that the removal of the 3′ nonhomologous end is blocked.

RAD1 has been implicated in endonucleolytic excision repair of UV photodimers, although its exact role has not been established (*10*–*12*). We propose that Rad1 protein could act as an endonuclease in the excision step of photodimer removal and in the removal of nonhomologous ends in DSB repair. In this view, DSB ends must be able to search for homology even when the ends of DNA are nonhomologous. One way that this could occur is by paranemic base-pairing of DNA, in which the invading strand is paired to its complementary partner but not interwound around it (*23*). Once such associations are formed, the *RAD1* gene product would be able to remove the nonhomology at the 3′ ends by cleaving off the nonhomologous segment, in a manner similar to the way in which a photodimer-containing "tail" must be removed from UV-damaged DNA before repair through new DNA replication can occur. An alternative possibility, that *RAD1* encodes a 3′ to 5′ exonuclease that could accomplish the same task, is less likely in light of both our genetic and physical experiments showing that HO-cut DNA produces 3′ tails that are almost never degraded, even when recombination is blocked (*5*, *24*).

This view of the role of *RAD1* helps explain most of its previously observed recombinational and repair phenotypes. First, *RAD1* would not be expected to play a major role in the repair of x-ray–induced DSBs, because most chromosomal lesions would be exactly homologous to an intact template (a sister chromatid or homolog). This same argument would also apply to HO-induced *MAT* switching, where one of the two ends of the DSB, the distal end, is exactly homologous to donor sequences at *HML* or *HMR*. Our results show that *RAD1* is necessary for gene conversion and SSA to proceed when nonhomologous DNA must be removed from the ends.

The absence of *RAD1* discourages SSA between direct repeats when a lesion is introduced in unique sequences between them. This may explain why *rad1* mutants reduce deletions but not gene conversions between heteroallelic direct repeats (*13*, *14*). This same effect can also account for a reduction in unequal sister-chromatid exchanges involving direct repeats if the initiating lesions occur in the sequences between the repeats.

We have also found a surprising appearance of lacZ triplication products in *rad1* strains. Such triplications are difficult to explain as alternative outcomes of a gap-repair intermediate when there is only one intact donor and where most cells contain only one copy of the plasmid (*7*). We favor a mechanism by which triplications arise by an alternative processing of recombination intermediates that contain 3′ tails, which otherwise would be removed by Rad1 protein (Fig. 4). The key step involves strand realignments similar to those proposed to occur during replication of retroviruses (*25*). Amplification of sequences within a repeated array could also

occur by this mechanism. Moreover, a strand realignment step occurring during SSA can lead to the formation of apparent gene conversion products, with two copies of the repeated sequences, unassociated with crossing-over.

REFERENCES AND NOTES

1. B. Connolly, C. I. White, J. E. Haber, *Mol. Cell. Biol.* **8**, 2342 (1988).
2. J. N. Strathern *et al.*, *Cell* **31**, 183 (1982).
3. R. Kostriken, J. N. Strathern, A. J. Klar, J. B. Hicks, F. Heffron, *ibid.* **35**, 167 (1983).
4. R. Kostriken and F. Heffron, *Cold Spring Harbor Symp. Quant. Biol.* **49**, 89 (1984).
5. C. I. White and J. E. Haber, *EMBO J.* **9**, 663 (1990).
6. N. Rudin and J. E. Haber, *Mol. Cell. Biol.* **8**, 3918 (1988).
7. N. Rudin, E. Sugarman, J. E. Haber, *Genetics* **122**, 519 (1989).
8. N. Sugawara and J. E. Haber, *Mol. Cell. Biol.* **12**, 563 (1992).
9. J. Fishman-Lobell, N. Rudin, J. E. Haber, *ibid.*, p. 1292.
10. R. J. Reynolds and E. C. Friedberg, *J. Bacteriol.* **146**, 692 (1981).
11. D. R. Wilcox and L. Prakash, *ibid.* **148**, 618 (1981).
12. R. D. Miller, L. Prakash, S. Prakash, *Mol. Cell. Biol.* **2**, 939 (1982).
13. H. Klein, *Genetics* **120**, 367 (1988).
14. B. J. Thomas and R. Rothstein, *ibid.* **123**, 725 (1989).
15. B. R. Zehfus, A. D. McWilliams, Y.-H. Lin, M. F. Hoekstra, R. L. Keil, *ibid.* **126**, 41 (1990).
16. R. H. Schiestl and S. Prakash, *Mol. Cell. Biol.* **8**, 3619 (1988).
17. Densitometric quantitation of the bands showed a fourfold reduction in the amount of deletion product. If gene conversion products were also decreased by fourfold, they should still represent 2% of the total DNA. We can readily detect this amount of gene conversion (*9*).
18. J. Fishman-Lobell and J. E. Haber, unpublished data.
19. R. Snow, *Mutat. Res.* **6**, 409 (1968).
20. J. Fishman-Lobell, thesis, Brandeis University (1992).
21. B. Weiffenbach *et al.*, *Proc. Natl. Acad. Sci. U.S.A.* **80**, 3401 (1983).
22. A G-test was used as described in R. R. Sokal and F. J. Rolf, in *Biometry* (Freeman, San Francisco, CA, 1969), pp. 599–600.
23. B. C. Schutte and M. M. Cox, *Biochemistry* **26**, 6516 (1987).
24. B. L. Ray, C. I. White, J. E. Haber, *Mol. Cell. Biol.* **11**, 5372 (1991).
25. E. Gilboa, S. W. Mitra, S. Goff, D. Baltimore, *Cell* **18**, 93 (1979).

26. We thank R. Keil who provided plasmid pL962, which contains a *LEU2* marked deletion of *RAD1*. We are grateful for the comments and suggestions of S. Lovett, L. Symingtom, M. Rosbash, N. Sugawara, and M. Lichten. Supported by NIH grant GM20056 and by predoctoral Genetics Training Grant GM01722.

6 May 1992; accepted 28 July 1992

Interaction of the Immunosuppressant Deoxyspergualin with a Member of the Hsp70 Family of Heat Shock Proteins

Steven G. Nadler,*† Mark A. Tepper,* Bernice Schacter,‡ Charles E. Mazzucco

Deoxyspergualin (DSG) is a potent immunosuppressant whose mechanism of action remains unknown. To elucidate its mechanism of action, an intracellular DSG binding protein was identified. DSG has now been shown to bind specifically to Hsc70, the constitutive or cognate member of the heat shock protein 70 (Hsp70) protein family. The members of the Hsp70 family of heat shock proteins are important for many cellular processes, including immune responses, and this finding suggests that heat shock proteins may represent a class of immunosuppressant binding proteins, or immunophilins, distinct from the previously identified *cis-trans* proline isomerases. DSG may provide a tool for understanding the function of heat shock proteins in immunological processes.

Deoxyspergualin (DSG) is a synthetic analog of spergualin, a natural product isolated from *Bacillus laterosporus* that possesses potent immunosuppressive activity (*1*–*6*). In many models of T cell–dependent immune responses, such as antibody production, delayed-type hypersensitivity, and allograft rejection, DSG exerts potent immunosuppressive effects (*2*, *3*, *7*). The mechanism of action of DSG is believed to be different from that of the immunosuppressants cyclosporin A and FK506. Unlike cyclosporin A and FK506, DSG does not alter the amount of interleukin-2 (IL-2) produced in response to T cell activation (*2*, *5*), and the time course of inhibition of the mixed lymphocyte response for DSG differs from that for cyclosporin A (*5*, *7*, *8*). Furthermore, in contrast to cyclosporin A, the effect of DSG on the generation of secondary cytotoxic T lymphocytes cannot be reversed with exogenous IL-2 (*5*). In an attempt to elucidate the mechanism of action of DSG, we have isolated a 70-kD intracellular DSG binding protein and identified this protein as a member of the Hsp70 family of heat shock proteins. This finding provides evidence for a class of immunophilins distinct from the previously identified *cis-trans* proline isomerases (*9*–*13*) that bind cyclosporin A and FK506.

Jurkat cell (human T cell) lysates were subjected to chromatography on a methoxy DSG-Sepharose column (Fig. 1). Methoxy DSG (Me-DSG) was used because it is more stable to hydrolysis than DSG but still possesses similar immunosuppressive activity (*7*, *14*). After application of the Jurkat cell lysate, the column was washed with a low- to high-salt gradient. On the subsequent application of 5 mM DSG, one major protein with an apparent molecular mass of 70 kD was specifically eluted. Only a small amount of the 70-kD protein was eluted from the column by the polyamines putrescine and spermidine, which have limited structural similarity to DSG and are not immunosuppressive (Fig. 2). Furthermore, the 70-kD protein did not bind to resin that did not contain DSG and was retained on the affinity column in the presence of 2 M NaCl or 0.5% Nonidet P-40, which suggests that the protein and affinity matrix interact with high affinity. In addition to Jurkat cells, we have identified the 70-kD protein in THP-1 cells (human monocytic), calf spleen cells, and thymus cells, as well as nonhematopoietic HeLa cells.

To identify the 70-kD protein, we subjected the affinity-purified protein to trypsin digestion, and the resulting peptides were separated by reversed-phase high-performance liquid chromatography (HPLC) (*15*). Several fractions from the HPLC-purified tryptic digest were chosen for amino acid sequencing. Although some fractions contained more than one peptide, we could unambiguously identify the sequences of six peptides (*16*). Each of the sequences of the DSG binding protein matched identically the sequence of the human constitutive heat shock cognate 70 (Hsc70) heat shock protein (*15*, *16*). Although there is an 81% sequence identity between the inducible Hsp70 heat shock protein and Hsc70, there are six amino acid differences between the peptide sequences of the DSG binding protein and inducible Hsp70 (*16*). These data identify the DSG binding protein as the constitutive or cognate member of the Hsp70 heat shock protein family.

To confirm the sequencing results, we also determined whether monoclonal antibodies to Hsp70 recognized the affinity-purified 70-kD protein (Fig. 3). Three different monoclonal antibodies, 7.10, 3a3, and N27F3-4, that recognize different epitopes found on both the constitutive and inducible Hsp70 proteins (*17*) each bound

Bristol-Myers Squibb Pharmaceutical Research Institute, Wallingford, CT 06492.

*Present address: Bristol-Myers Squibb Co., Seattle, WA 98121.
†To whom correspondence should be addressed.
‡Present address: Biotransplant Inc., Charlestown, MA 02129.